P1.5

COMPARISON OF THE ADVANCED VERY HIGH RESOLUTION RADIOMETER (AVHRR) AND MODERATE RESOLUTION IMAGING SPECTRORADIOMETER (MODIS) CLOUD PROPERTIES USING PATMOS-X

William C. Straka III[+], Andrew K. Heidinger*

[+] Space Science and Engineering Center, University of Wisconsin at Madison, Madison, WI

*Office of Research and Applications, NOAA/NESDIS, Madison, Wisconsin

1. INTRODUCTION

The transition to more advanced instruments in the national polar and geostationary satellite imagers (VIIRS and ABI) from the current set of imagers (AVHRR and GOES), the remote sensing capabilities of clouds will certainly improve. Data from the current operational sensors, primarily AVHRR, has provided roughly 30 years of data. This comprises the bulk of the satellite data used to understanding decadal cloud variability. In order to make cloud climatologies from the operational sensors relevant to those of the upcoming advanced sensors, research and analysis are required to develop methods to make physically consistent climate data record from both the current and future sensors. In this paper, we explore the consistency in the cloud optical depth and particle records from the AVHRR and GOES imagers and those derived from the additional channels offered by MODIS, through the use of the MODIS instrument and the AVHRR cloud optical properties algorithm. The physical basis for the observed differences will be demonstrated and propose methods to make the time series more consistent.

The motivation for this research comes from our desire to make continuous cloud climate climatologies from the AVHRR/MODIS. VIIRS will be the successor to the AVHRR as the imager on NOAA's operational polar orbiters. VIIRS will offer similar channels to cloud remote sensing as MODIS. The AVHRR processing done here was done within the AVHRR Pathfinder Extended Project (PATMOS-x) which is a pilot study conduced with the NOAA/NESDIS Office of Research and Applications. PATMOS-x is a new version of PATMOS (Jacobowitz et al., 2004). Unlike PATMOS, PATMOS-x includes a full suite of cloud properties that are similar to those produced by MODIS.

For this initial study, we are focusing on the optical thickness and particle size of oceanic stratus. Because of the known surface reflectance of the ocean and the lack of uncertainty in particle shape, we feel that achieving consistency between AVHRR and MODIS for oceanic stratus is reasonable first step. The variation in ice crystal shapes and their scattering properties offers additional complications are the comparison of ice cloud properties. While our primary focus is on oceanic stratus clouds, we intend to extend this work to other cloud properties and other regions.

This study will compare optical depth and cloud effective radius measurements from MODIS radiance data using algorithms developed for PATMOS-x dataset to the MODIS Joint Level 2 data (King et al., 1998). In addition, monthly averaged data from MODIS Level 2 data will be compared with monthly averaged data from the PATMOS-x dataset. This data begins in 1982 and goes through the current set of NOAA polar orbiters and NASA satellites. This will help in creating an algorithm that can be used on future operational and research satellites. In addition, it will help in doing climatological studies of important physical properties of clouds, such as optical depth and cloud effective radii.

2. DATA AND METHODOLOGY

MODIS level 1b reflectance and brightness temperatures at 5km resolution data were used in conjunction with the PATMOS-x cloud optical depth and cloud effective radius algorithms. Lookup tables were generated for channels 1 and 20, which correspond to AVHRR channels 1 and 3b (.6 and 3.7 μm). Data corresponding to AVHRR channel 3a (1.6 μm), which corresponds to MODIS channel 6, was not used. This is because the 3a channel on AVHRR was not implemented until after NOAA 15. So, for a consistent dataset, only the data from the 3b channel can be considered.

The 5km AQUA MODIS Level 1b data were used because it was being compared to the AQUA MOD06 optical depth and effective radius data. These data were used to compare with the PATMOS-x derived quantities. In addition, the MOD06 cloud phase product was used to determine the phase of each pixel, thus determining which forward model to use in the PATMOS-x algorithm. Finally, PATMOS-x and the MODIS MOD08 monthly mean optical depth and effective radius data were used.

Because imagers, particularly those in the solar IR (SIR) are sensitive to cloud phase as well as particle size, MODIS granules of oceanic stratus clouds because they consist of water particles were selected for the initial test of this comparison. The sensitivity of the SIR to cloud phase and particle size is why the MODIS optical depth and effective radius routines use a combination of seven channels in the 0.66 to 11μm (King *et al*., 1998).

*Corresponding author address: W.C. Straka III, Space Science and Engineering Center, Cooperative Institute for Meteorological Satellite Studies, 1225 West Dayton Street, Madison, WI 53706; Fax: (608) 262-5974; e-mail: wstraka@ssec.wisc.edu

3. ANALYSIS

Data from several MODIS granules were analyzed for this study. While only one case is shown in this paper, the other granules gave similar results. This particular granule was located in the south central Pacific Ocean, located between –31.40 and –10.38 latitude and –125.99 and –99.20 longitude taking place on 18 July 2005 with the 0010-2115 AQUA ascending node. The MODIS MOD06 optical depth routines (King et al., 1998) use a combination of the .6 (optical depth over land), 0.858 (optical depth over ocean), 1.240 (optical depth over snow/ice) while the PATMOS-x routine uses a single channel (.6 μm) to determine the optical depth. MODIS mainly uses the 2.13 μm channel to determine the optical depth (King et al., 1998), but occasionally uses or 3.75 and (when available) 1.6 μm to compute the effective radius. The last two channels are available on the AVHRR instruments as 3a and 3b, respectively. In order to see how the PATMOS-x algorithm performs compared to the MODIS algorithms, we will pass data from each of the three channels used by MODIS and compare the output. This will be done over oceanic clouds that primarily consist of water.

Because the wavelength used in the effective radii routines look at different depths into the cloud (Platnick, 2000), we expect there to be differences. In addition, we expect there to be some differences in the optical depth, as we are looking at oceanic clouds with a different channel than MODIS does. Unfortunately, the 1.6 μm channel on Aqua satellite did not function properly this channel is not used in the Aqua effective radius routine. Our goal here is to demonstrate that the difference are in agreement with theory. The development of techniques to remove these differences is ongoing.

Finally, a comparison with the monthly averaged AQUA MOD08 optical depth and effective radius for water particles is compared with PATMOS-x data from the AVHRR instrument on all NOAA morning and afternoon satellites (NOAA 7, 9, 11, 12, 14 and 15-18). Because the AVHRR instrument does not carry a 2.1 μm, it is expected that there is likely some difference

3.1 Optical depth

While the PATMOS-x optical depth algorithm does not use the three channels directly, the output from the effective radii part of the forward model are used to check for convergence. It was found that when the particular granule consisted of primarily liquid water clouds both the MODIS MOD06 (cloud product) and PATMOS-x derived optical depth tended to agree fairly well. The first figure is the comparison when using the 3.7 μm for the convergence test (Figure 1). Through out this section, the same shading applies for all of the plots. White means less than 10 points in that area, black means between 10 and 24 points, blue means between 25 and 49, cyan means between 50 and 99 points, yellow means between 100 and 149 points. Finally, red means that there are over 150 points in the shaded region.

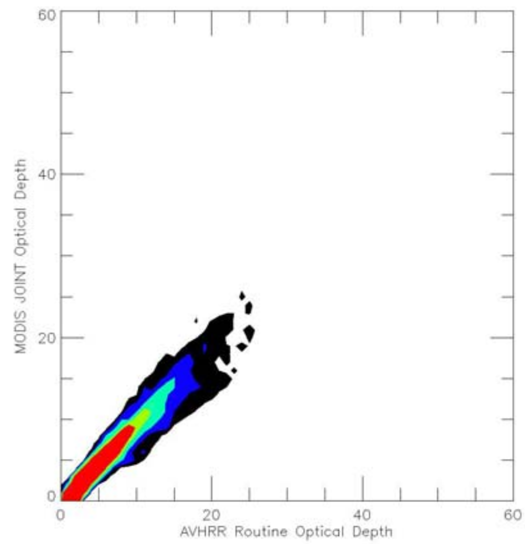

Figure 1. Optical depth using 3.7 μm from 22 July 2005, 2115 AQUA granule using PATMOS-x and MOD06 algorithms

As can be seen, the two optical depth routines tend to agree fairly well. There is not much scatter, especially at small optical depths. However, at larger optical depths, there is quite a bit of divergence. Figure 2 is the same PATMOS-x algorithm, except using the 2.1 μm channel effective radius as part of the convergence test.

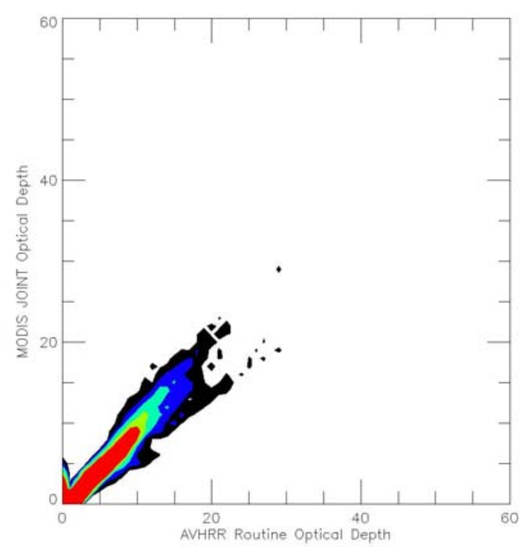

Figure 2. Optical depth for water particles using 2.1 μm data, from 22 July 2005, 2115 AQUA granule using PATMOS-x and MOD06 algorithms.

When using 2.1 μm in the convergence test, we get a similar looking relationship between the optical depth from PATMOS-x and the MOD06 data. However, there is some divergence to the data at smaller optical depths. This may be due to the way that the convergence test is handled. In addition, there is a larger amount of divergence at larger optical depths. This is possibly due to the spread of the effective radii for larger particles.

As can be seen through this example, the channel that is used in the convergence test in PATMOS-x affects how correlated the optical depth is. This is likely because the various channels see different depths into the cloud. The 3.7 μm channel, for example, only sees the top 100-200m of the cloud. In addition, it has the least dependence on cloud thickness, reaching a reflectance limit at around an optical depth of 5 (Plantick, 2000). The 2.1 μm channel, however, sees further in to the cloud and has a reflectance limit that is higher. This is possibly why there is some divergence at the low end of the optical depth between the two routines.

Overall, though, the PATMOS-x results using the 3.7 μm channel, AVHRR channel 3b and MODIS channel 20, had the best correlation with the MOD06 results. This is despite the fact that the MOD06 routine uses the 0.858 μm to calculate optical depths over ocean, while the PATMOS-x algorithm uses the .6 μm, used by MODIS to calculate optical depths over land, to calculate the optical depth.

3.2 Effective radius

While there was a relatively nice relationship between the PATMOS-x algorithm and the MODIS cloud properties algorithm for optical depth, there were differences that occurred when it came to the effective radius routine. These differences, however, did not seem to emerge that much when it came to the convergence tests used for the optical depth routine.

The MODIS MOD06 effective radius data were expected to be different than PATMOS-x data because the PATMOS-x routine uses a single channel. However, the MOD06 algorithm typically uses a combination of three separate channels. These channels have been found to look at a different part of the cloud, depending on the liquid water content as well as the solar and viewing angles. However, typically, the 3.7 μm channel typically looks at cloud top, the 2.1 μm channel looks typically sees the middle part of the cloud and the 1.6 μm channel typically sees particles in the lower part of the cloud (Platnick, 2000). Typically, for water clouds the effective radius of particles typically increases from cloud base to cloud top. This would result in the 3.75 μm retrieval being the most sensitive to drops high in the cloud and 1.64 μm much lower in the cloud.

Typically, the MOD06 routine uses the 2.1 μm channel to derive the cloud effective radius. The MODIS Collection 5 data is expected to include the 2.1-3.7 μm and 2.1-1.6 μm effective radii differences. This would allow for researchers to compare how effective radius changes through out a cloud. However, at the time of this study, no MODIS Collection 5 data was available. In addition, the 1.6 μm channel (equivalent to the AVHRR 3a channel) was damaged, so a comparison with that channel was not performed. Thus, a comparison between the MOD06 2.1 μm channel derived effective radii with the PATMOS-x routine for water particles using the 3.7 and 2.1 μm channels were performed. In addition to using these two different channels, we also limited our observations to optically thick ($\tau > 5$) clouds. The effective radius algorithm was performed on the same granules as the optical depth to provide a direct comparison.

Figure 3 is the comparison between the 2.1 μm MOD06 algorithm and the PAMTOS-x algorithm using the 2.1 reflectances. Because the two algorithms are using the same channel, they should be equivalent.

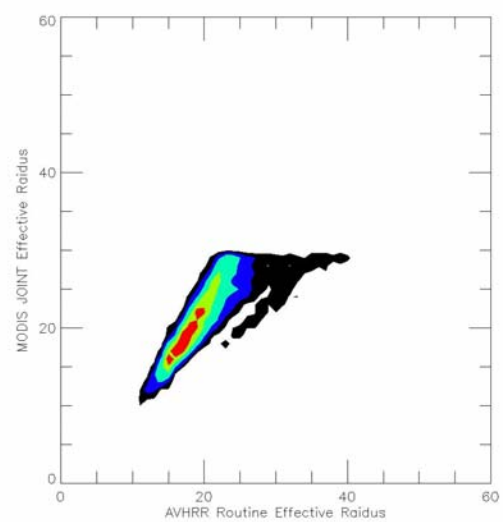

Figure 3. Effective radius comparison for water particles using 2.1 μm, from 21 July 2005, 2115 AQUA granule using PATMOS-x and MOD06 algorithms

As can be seen, the 2.1 μm PATMOS-x derived effective radius and the MOD06 derived effective radius are in moderate agreement. However, there are some differences. The first is that the MOD06 data seems to cut off at around 30 microns. This is likely due to the way the lookup tables are organized. In addition, larger water particles are typically not observed in maritime clouds. Finally, the PATMOS-x derived effective radius is not exactly the same as the MOD06 algorithm. While it is only slightly off, the differences are likely due to the way that the algorithm passes the reflectance data through as well as differences in the lookup tables used in the forward model. However, it is only slightly off an exact match.

Figure 4 is the comparison between the PATMOS-x and MOD06 algorithms for only water particles (as determined by the MOD06 cloud phase routine) using the 3.7 μm PATMOS-x derived effective radius.

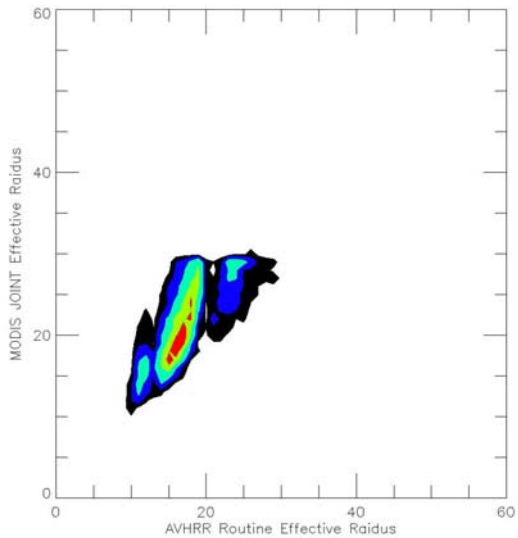

Figure 4. Effective radius comparison for water particles using 3.7 μm, from 21 July 2005, 2115 AQUA granule using PATMOS-x and MOD06 algorithms

As can be seen, the PATMOS-x derived effective radii are smaller than the MOD06 values. This is different than expected, as the 3.7 μm looks at a higher part of the cloud than the MOD06, 2.1 μm, effective radius algorithm does. This would mean that the 3.7 micron derived effective radius should be larger. Despite this difference, there is a cut off at around 30 microns for the MOD06 data.

3.3 PATMOS-x and MOD08 comparison

After a comparison between algorithms using similar scene data, monthly AVHRR derived liquid water optical depth and effective radius from the PATMOS-x data set with the AQUA MODIS monthly averaged liquid water optical depth and effective radius were compared. Figure 5 shows the comparison between the PATMOS-x and AQUA MODIS monthly averaged optical depths in a region of the south Pacific, just off the coast of South America.

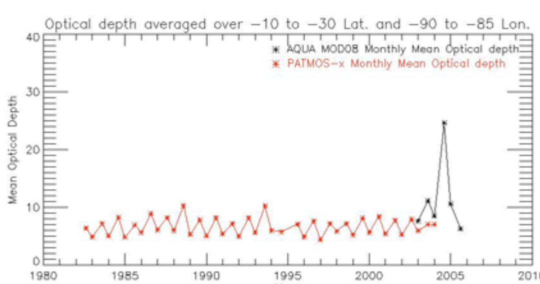

Figure 5. Comparison between the monthly averaged optical depth PATMOS-x data set using AVHRR data and the mothly avereaged optical depth from Aqua (MOD08) over a box off the northwestern South America.

The data (Figure 5) suggests that the PATMOS-x and the MODIS monthly averaged stratus optical depth data are fairly consistent, with the exception of one MODIS outlier in late 2004, the optical depth comparisons are similar to what were observed in the granules that were studied. However, because of the fact that MODIS has only been operating for a few years, no definite solutions can be drawn from this comparison just yet.

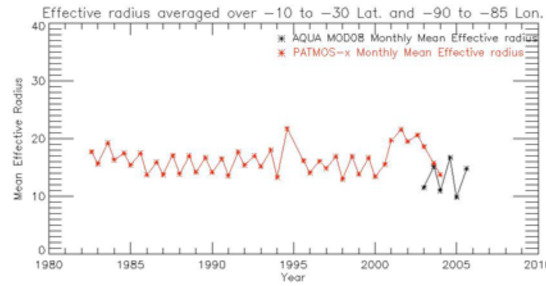

Figure 6. Comparison between the monthly averaged optical depth PATMOS-x data set using AVHRR data and the monthly averaged optical depth from Aqua (MOD08) over a box off the northwestern South America.

The effective radius comparisons using monthly averaged AVHRR data and MODIS data (Figure 6) are different than those observed in the granule comparisons. The data that is available suggests that the PATMOS-x effective radius, using the AVHRR, is slightly larger than the effective radii from the AQUA MODIS cloud product. It should be noted that during 2002-2003, NOAA-16 operated with the 1.6 μm channel replacing the 3.75 μm channel. This corresponds to the period in Figure 6 of increased in effective radius. This increase goes against the argument that the 1.6 μm channels sees the deepest into the cloud, thus producing the smallest estimate of effective radius. While this discrepancy is currently being investigated, one potential culprit is the calibration of the 1.6 μm channel on the NOAA-16 AVHRR.

The MODIS data seems to be more consistent with the average maritime cloud effective radius than the PATMOS-x monthly mean. On average, an oceanic maritime cloud in the tropics typically has a cloud effective radius of around 12 microns, especially for optically thick clouds (Han 1994). The PATMOS-x analysis seems to give a slightly higher average cloud effective radius, roughly around 15 microns, while the monthly averaged MODIS data gives a cloud effective radius of around 12 microns. This might be due to the differences in the channel that is used, as the AVHRR 3b channel is 3.7 μm, while MODIS uses the 2.1 μm channel. When the MODIS collection 5 data becomes available, a better analysis will be able to be performed.

4. CONCLUSIONS

This study compared two sets of data. First, the optical depth and cloud effective radius measurements from MODIS radiance data using algorithms developed for PATMOS-x dataset to the MODIS Joint Level 2 data were compared from several MODIS granules. Granules containing primarily liquid water oceanic stratus clouds were due to the uniformity of the cloud. It was found that the MOD06/JOINT optical depth was roughly the same as the optical depth calculated using the PATMOS-x algorithm. This was the case even when ice particles were included in analysis.

However, the effective radius that was calculated from the PATMOS-x algorithm. It was found that there was a bias towards slightly larger particles when using the PATMOS-x routine compared to the MOD06 data. The difference is likely due to spectral differences in the channels used in the algorithms. In addition, when looking at only water particles, as determined by the MOD06 data, the MOD06 effective radius seems to have a cut off at around 30 microns, likely due to the way the lookup tables in the MOD06 routine are set up. This supported by the fact that, when the PATMOS-x routine looked at both ice and water particles, the cut off seems to disappear and comes into better agreement with the MOD06 data.

The idea that different spectral bands provide different information regarding the cloud is supported by this study. The relationship between the two routines acts very differently whether the 2.1μm, which is what the MOD06 algorithm uses to determine the effective radius, or the 3.75 μm channel is being used in the PATMOS-x routine. A comparison with the MODIS 3.75 μm algorithm was not performed, as it is not included in the Collection 4 JOINT dataset.

The second data set studied was monthly averaged data from MODIS Level 2 data compared with monthly averaged data from the PATMOS-x dataset. This data begins in 1982 and goes through the current set of NOAA polar orbiters and NASA satellites. Data averaged over a region similar to the one used in the granule comparison was performed. The annual cycle in both the optical depth and effective radius, with the exception of a few outliers, was present in all of the data. Much like the comparison with the granule level data, the two sets of optical depths were nearly consistent. This is likely due to the fact that both the MODIS and PATMOS-x algorithms use roughly the same wavelength channel, .63 μm, to calculate the optical depth. Some difference may be explained by the fact that the MODIS routine uses the .858 μm channel to calculate the optical depth over the ocean.

The monthly averaged effective, however, was different in that the monthly averaged PATMOS-x routine measured higher effective radii than the monthly averaged MODIS data. On average, an oceanic maritime cloud in the tropics typically has a cloud effective radius of around 12 microns, especially for optically thick clouds (Han 1994). The monthly averaged MOD06 data tends to agree with this average effective radius, while the PATMOS-x dataset gives a slightly higher effective radius. This can possibly be attributed to the different spectral bands that are used in the MODIS level data.

Future studies of this project will include looking at MODIS and PATMOS-x data over land as well as comparing data at surface observation sites in the United States and else where, including ARM or SURFRAD sites. Also, it is hoped that this dataset can be used in an inter-satellite comparison of cloud property measurements, especially between the PATMOS-x and GOES datasets. GOES allows for near real-time data analysis from Japan (GOES-09) through the eastern Atlantic (GOES-12). Finally, a comparison with the MOD06 Collection 5 data, when it becomes available, will be performed. A correction to remove spectral dependence on r_e estimation for water clouds is necessary to develop. This is because, as has been stated previously, the various channels used in the both MODIS and AVHRR have been shown to look at different depths of the cloud. While this can be useful in looking at the vertical variations of the cloud drop effective radii (Chang and Li, 2002). In order to account for the vertical variations in effective radius due to the influence of the spectral dependence of the effective radius algorithms, we must fully understand the dependencies and correct for them. While the optical depth measurement is dependant on wavelength, a correction is not necessary as a standard channel, namely the visible channel, is already used between various satellites.

Acknowledgements: This research was supported by the NOAA/NESDIS Office of Research and Applications (ORA).

6. REFERENCES

Pavolonis, M.J., and J.R. Key, 2003: Antarctic cloud radiative forcing at the surface estimated from the AVHRR Polar Pathfinder and ISCCP D1 datasets, 1985-93. *J. Appl. Meteor.*, **42**, 827-840

Han, Q., W.B. Rossow, A. A. Lacis, 1994. Near-Global Survey of Effective Droplet Radii in Liquid Water Clouds Using ISCCP Data, *J. Climate*, **7,** 465-497.

Jacobowitz, H., L. L. Stowe, G. Ohring, A. K. Heidinger, K. Knapp, N. R. Nalli, 2003. The Advanced Very High Resolution Radiometer Pathfinder Atmosphere (PATMOS) Climate Dataset: A Resource for Climate Research *Bull. Amer. Meteor. Soc.*, **84**, 785-793.

King, M. D., S-C Tsay, S. E. Platnick, M. Wang and K-L. Liou, 1998: Cloud Retrieval Algorithms for MODIS: Optical Thickness, Effective Particle Radius, and Thermodynamic Phase. Products: 06_L2, 08_D3, 08_E3, 08_M3. ATBD Reference Number: ATBD-MOD-05.

Chang, F.-L., and Z. Li, 2002. Estimating the vertical variation of cloud droplet effective radius using multispectral near-infrared satellite measurements, *J. Geophys. Res.*, **107**, 1 – 12

Le Marshall, J., A. Rea, J. Jung, J. Daniels and M. Dunn, 2004: Error Characterization and Application of Atmospheric Motion Vectors. *Proceedings of the Seventh International Winds Workshop* 14-17 June 2004, Helsinki, Finland.

Platnick, S., 2000. Vertical photon transport in cloud remote sensing problems, *J. Geophys. Res.*, **105**(D18), 22919-22936.

Wylie, D. P., and W. P. Menzel, 1989: Eight years of high cloud statistics using HIRS. *J. Climate*, **12**, 170–184.